

ExoMol molecular line lists XIX: high accuracy computed hot line lists for H_2^{18}O and H_2^{17}O

Oleg L. Polyansky^{1,2}, Aleksandra A. Kyuberis², Lorenzo Lodi¹, Jonathan Tennyson^{1*}, Sergei N. Yurchenko¹, Roman I. Ovsyannikov², and Nikolai F. Zobov²

¹Department of Physics and Astronomy, University College London, London WC1E 6BT, UK

²Institute of Applied Physics, Russian Academy of Sciences, Ulyanov Street 46, Nizhny Novgorod, Russia 603950.

Accepted XXXX. Received XXXX; in original form XXXX

ABSTRACT

Hot line lists for two isotopologues of water, H_2^{18}O and H_2^{17}O , are presented. The calculations employ newly constructed potential energy surfaces (PES) which take advantage of a novel method for using the large set of experimental energy levels for H_2^{16}O to give high quality predictions for H_2^{18}O and H_2^{17}O . This procedure greatly extends the energy range for which a PES can be accurately determined, allowing accurate prediction of higher-lying energy levels than are currently known from direct laboratory measurements. This PES is combined with a high-accuracy, *ab initio* dipole moment surface of water in the computation of all energy levels, transition frequencies and associated Einstein A coefficients for states with rotational excitation up to $J = 50$ and energies up to $30\,000\,\text{cm}^{-1}$. The resulting HotWat78 line lists complement the well-used BT2 H_2^{16}O line list (Barber et al. 2006, MNRAS, **368**, 1087). Full line lists are made available in the electronic form as supplementary data to this article and at www.exomol.com.

Key words: molecular data; opacity; astronomical data bases: miscellaneous; planets and satellites: atmospheres; stars: low-mass; stars: brown dwarfs.

1 INTRODUCTION

Water spectra can be observed from many different regimes in the Universe, several of which are discussed further below. The spectrum of water, particularly at elevated temperatures, is rich and complex. A few years ago Barber et al. (2006) presented a comprehensive line list, known as BT2, which used well-established theoretical procedures to compute all the transitions of H_2^{16}O of importance in objects with temperatures up to 3000 K. BT2 contains about 500 million lines. A similar line list for HD^{16}O , known as VTT, was subsequently computed by Voronin et al. (2010).

The BT2 line list has been extensively used. It forms the basis of the most recent release of the HITEMP high-temperature spectroscopic database (Rothman et al. 2010) and for the BT-Settl model (Allard 2014) for stellar and substellar atmospheres covering the range from solar-mass stars to the latest-type T and Y dwarfs. BT2 has been used to detect and analyse water spectra in objects as diverse as the Nova-like object V838 Mon (Banerjee et al. 2005), atmospheres of brown dwarfs (Rice et al. 2010) and M subdwarfs (Rajpurohit et al. 2014), and extensively for exoplanets (Tinetti et al. 2007; Birkby et al. 2013). Within the solar system BT2 has been used to show an imbalance between nuclear spin and rotational temperatures in cometary comae (Dello Russo et al. 2004, 2005) and assign a new set of, as yet unexplained, high energy water emissions in comets (Barber et al. 2009), as well as to model water spectra in the deep atmosphere of Venus (Bailey 2009).

Although BT2 was developed for astrophysical use, it has been applied to a variety of other problems including the calculation of the refractive index of humid air in the infrared (Mathar 2007), high speed thermometry and tomographic imaging in gas engines and burners (Kranendonk et al. 2007; Rein & Sanders 2010), as the basis for an improved theory

* Email: j.tennyson@ucl.ac.uk

of line-broadening (Bykov et al. 2008), and to validate the data used in models of the earths atmosphere and in particular simulating the contribution of weak water transitions to the so-called water continuum (Chesnokova et al. 2009).

There are several water line lists published in the literature (Viti et al. 1997; Partridge & Schwenke 1997; Barber et al. 2006; Mikhailenko et al. 2005). Two linelists have also been computed specifically for the isotopologues: Shirin et al. (2008) created the 3mol room-temperature line lists for H_2^{16}O , H_2^{17}O and H_2^{18}O based on the PES of Shirin et al. (2006); Tashkun created a number of line lists based on the work of Partridge & Schwenke (1997), see Mikhailenko et al. (2005). These are considered further below.

At present hot line lists are only published for H_2^{16}O and HD^{16}O . However isotopically-substituted water containing ^{18}O or ^{17}O provides important markers for a variety of astronomical problems (Nittler & Gaidos 2012). For example Matsuura et al. (2014) recently detected H_2^{18}O in the emission-line spectrum of the luminous M-supergiant VY CMa. Astronomical spectra of water isotopologues (Neufeld et al. 2013) and their direct analysis in cometary dust particles (Floss et al. 2010) and carbonaceous chondrites (Clayton & Mayeda 1984; Vollmer et al. 2008) have been used to determine formation mechanisms and constrain formation models. Water isotope ratios are also used to monitor stellar evolution (Abia et al. 2012) and to probe the atmosphere of Mars (Villanueva et al. 2015). The seemingly minor isotopologues of water can be important species in their own right with, for example, H_2^{18}O being the fifth largest absorber of sunlight the earth's atmosphere.

There is therefore a need for line lists equivalent to BT2 for H_2^{17}O and H_2^{18}O to aid spectroscopic studies, and it is these that are presented here. These lists form part of the ExoMol project (Tennyson & Yurchenko 2012) which aims to provide a comprehensive set of molecular line lists for studies of molecular line lists for exoplanet and other hot atmospheres.

Although our new line lists in some way mimic BT2, they also take advantage of a number of recent theoretical developments. In particular a IUPAC task group (Tennyson et al. 2014) used a systematic procedure (Furtenbacher et al. 2007) to derive empirical energy levels for all the main isotopologues of water (Tennyson et al. 2009, 2010, 2013, 2014). These levels are combined with a newly-developed procedure for enhancing the accuracy of calculations on isotopically substituted species, which is used for the first time here. This ensures that most of the key frequencies in our new line lists are determined with an accuracy close to experimental, even though many of them are yet to be observed. Furthermore, theoretical work on improving the accuracy and representation of the water dipole moment (Lodi et al. 2008, 2011) has improved the accuracy with which water transition intensities are predicted (Grechko et al. 2009). Some of these advances have already been used to create improved room temperature line lists for H_2^{17}O and H_2^{18}O (Lodi & Tennyson 2012) which were included in their entirety in the 2012 release of HITRAN (Rothman L. S. et al. 2013).

The paper is structured as follows: section 2 outlines our overall methodology and presents the derivation of potential energy surfaces (PES). The details of the calculation of the new line lists, along with comparison with previous line lists, are given in section 3. Section 4 discusses further improvement of the line list by the substitution of calculated energy levels with empirical ones, together with the procedure used to label energy levels with approximate vibrational and rotational quantum numbers. Our results are discussed in section 5.

2 POTENTIAL ENERGY SURFACES

The fitting of water (H_2^{16}O) PESs to experimental spectroscopic data has a long history. The first fitted PES giving near to experimental accuracy was PJT1 (Polyansky et al. 1994). Partridge & Schwenke (1997) constructed a fitted PES starting from a highly accurate *ab initio* calculation; all subsequent water potentials followed this procedure and have been based on *ab initio* studies of increasing sophistication. As a result there are several very good water PESs available (Shirin et al. 2003, 2008; Bubukina et al. 2011).

Here we need a PES which satisfies two criteria. First, it should be at least as accurate as the PES used for the BT2 line list with the calculated energies ranging up to 30 000 cm⁻¹. Second, the PES should be adapted to the calculation of energy levels of the two water isotopologues H_2^{17}O and H_2^{18}O . This second requirement is harder to fulfill, as the characterisation of the experimental energy levels of both H_2^{17}O and H_2^{18}O is significantly less extensive than for H_2^{16}O (Tennyson et al. 2014).

To take advantage of the accumulated knowledge on the spectrum H_2^{16}O in constructing a PES for H_2^{17}O and H_2^{18}O and following previous work (Zobov et al. 1996; Voronin et al. 2010; Bubukina et al. 2011), we decided to fit a Born-Oppenheimer (BO) mass-independent PES to the available data for H_2^{16}O and fix the adiabatic BO diagonal correction (BODC), mass-dependent surface to the *ab initio* value of Polyansky et al. (2003). Obviously this procedure requires the accuracy of predictions for H_2^{17}O and H_2^{18}O to be verified. This is done by comparing the calculated H_2^{17}O and H_2^{18}O energy levels to the available experimentally-determined ones (Tennyson et al. 2009, 2010).

We used the same fitting procedure as Bubukina et al. (2011). Nuclear motion calculations were performed with DVR3D (Tennyson et al. 2004). As elsewhere, in the fit the experimentally derived energies of H_2^{16}O for the $J = 0, 2$ and 5 rotational states by Tennyson et al. (2013) were used.

In the following our new empirical PES obtained using the fitting procedure described above will be referenced to as PES1, while the PES by Bubukina et al. (2011) will be referenced to as PES2. Tables 1 and 2 present a comparison between

Table 1. Comparison of calculated $J = 0$ term values for $H_2^{17}O$ using three potentials with experimental data. Experimental (obs) data is taken from Tennyson et al. (2009).

v_1	v_2	v_3	Observed	PES1	Obs.-Calc.	PES2	Obs.-Calc.	PES3	Obs.-Calc.
0	0	1	3748.318	3748.334	-0.02	3748.326	-0.01	3748.463	-0.15
0	0	2	7431.076	7431.103	-0.03	7431.059	0.02	7431.467	-0.39
0	0	3	11011.883	11011.936	-0.05	11011.860	0.02	11012.268	-0.38
0	1	0	1591.326	1591.297	0.03	1591.342	-0.02	1591.413	-0.09
0	1	1	5320.251	5320.241	0.01	5320.251	0.00	5320.378	-0.13
0	1	2	8982.869	8982.868	0.00	8982.844	0.03	8983.118	-0.25
0	1	3	12541.227	12541.267	-0.04	12541.207	0.02	12541.614	-0.39
0	2	0	3144.980	3144.934	0.05	3144.993	-0.01	3145.085	-0.10
0	2	1	6857.273	6857.260	0.01	6857.266	0.01	6857.476	-0.20
0	7	1	13808.273	13808.224	0.05	13808.371	-0.10	13809.171	-0.90
1	0	0	3653.142	3653.147	0.00	3653.121	0.02	3653.193	-0.05
1	0	1	7238.714	7238.773	-0.06	7238.726	-0.01	7238.932	-0.22
1	0	2	10853.505	10853.545	-0.04	10853.504	0.00	-	-
1	0	3	14296.280	14296.340	-0.06	14296.265	0.01	14296.584	-0.30
1	1	0	5227.706	5227.691	0.01	5227.704	0.00	5227.881	-0.18
1	1	1	8792.544	8792.578	-0.03	8792.546	0.00	8792.816	-0.27
1	2	0	6764.726	6764.747	-0.02	6764.722	0.00	6764.905	-0.18
1	2	1	10311.202	10311.247	-0.05	10311.199	0.00	10311.421	-0.22
1	3	1	11792.822	11792.861	-0.04	11792.834	-0.01	11793.172	-0.35
2	0	0	7193.246	7193.265	-0.02	7193.257	-0.01	7193.394	-0.15
2	0	1	10598.476	10598.550	-0.07	10598.483	-0.01	10598.763	-0.29
2	1	1	12132.993	12133.056	-0.06	12132.984	0.01	12132.365	0.63
2	2	1	13631.500	13631.542	-0.04	13631.489	0.01	13631.650	-0.15
3	0	1	13812.158	13812.215	-0.06	13812.170	-0.01	13812.394	-0.24
3	2	1	16797.168	16797.182	-0.01	16797.177	-0.01	16797.011	0.16
4	0	1	16875.621	16875.662	-0.04	16875.643	-0.02	16875.474	0.15

the $J = 0$ energy levels calculated using PES1, PES2 for $H_2^{17}O$ and $H_2^{18}O$ respectively. For comparison as a third column we present the $J = 0$ levels and corresponding discrepancies using the PES (called PES3 in the tables) due to Partridge & Schwenke (1997) taken from the linelist calculated by Dr. S.A. Tashkun and summarised by Mikhailenko et al. (2005). The line list based on PES3 was calculated for three temperatures: T=296 K, 1000 K and 3000 K. For all versions the highest value of the rotational quantum number J considered is 28 and the spectral range is 0-28500 cm⁻¹. The number of lines for $H_2^{18}O$ is 108 784 and for $H_2^{17}O$ 109 083.

Indeed, one can see that the agreement with the experiment is very good. Although the results obtained using PES2 are somewhat better than those for PES1. However employing PES1 gives us the opportunity to use the information on $H_2^{16}O$ experimental energy levels to predict very accurately energy levels of $H_2^{17}O$ and $H_2^{18}O$. We call these predicted levels pseudo-experimental energies for the reasons explained below. Table 3 illustrates the unprecedented accuracy of the prediction of the $H_2^{17}O$ energy levels for those states whose energies are known experimentally. The slightly less good, but still very accurate, energy levels predicted for $H_2^{18}O$ are shown in the column 2 of Table 3. We might expect a similar level of accuracy for predictions of the $H_2^{17}O$ and $H_2^{18}O$ energy levels for states yet to be measured for these isotopologues, but known for $H_2^{16}O$. We note that the standard deviations given in Table 3 are rather systematic suggesting that further improvement in the predictions may be possible. This and details of our final pseudo-experimental energy levels are discussed in section 4.

Recently, highly lying energy levels of $H_2^{18}O$ have been measured using multiphoton spectroscopy (Makarov et al. 2015). These levels lie at about 27 000 cm⁻¹ and therefore provide a stringent test of our procedure. The highest upper energy level considered in this work, as for BT2, is 30 000 cm⁻¹; Table 4 illustrates the high quality of our calculations over the whole range considered. In fact recent studies confirm that BT2 is not so accurate for these high energy states (Lampel et al. 2016).

Thus, the line lists, details of whose calculations are given in the following section, are computed using a higher quality PES than that used to compute BT2. Three sets of energy levels are provided as part of this line list. The first set is the variationally calculated energy levels obtained using PES2. The second set comprises these energy levels substituted by the experimental values (Tennyson et al. 2009) where available. The third set is further with pseudo-experimental energy levels substituted whenever $H_2^{16}O$ experimental energy levels (Tennyson et al. 2013) are available (see below). This third set is the one we recommend for creating spectra with HotWat78 because of its increased accuracy.

3 LINE LIST CALCULATIONS FOR $H_2^{17}O$ AND $H_2^{18}O$

The line list calculations were performed with the DVR3D program suite (Tennyson et al. 2004) using the PES1 and PES2 discussed above, and the *ab initio* dipole moment surfaces LTP2011S of Lodi et al. (2011). As for BT2, the highest rotational

Table 2. Comparison of calculated $J = 0$ term values for H_2^{18}O using three potentials with experimental data. Experimental (obs) data is taken from Tennyson et al. (2009).

v_1	v_2	v_3	Observed	PES1	Obs.-Calc.	PES2	Obs.-Calc.	PES3	Obs.-Calc.
0	0	1	3741.57	3741.581	-0.01	3741.567	0.00	3741.575	-0.01
0	0	2	7418.72	7418.741	-0.02	7418.693	0.03	7418.759	-0.03
0	0	3	10993.68	10993.734	-0.05	10993.659	0.02	10993.689	-0.01
0	1	0	1588.28	1588.240	0.04	1588.271	0.00	1588.299	-0.02
0	1	1	5310.46	5310.443	0.02	5310.438	0.02	5310.388	0.07
0	1	2	8967.57	8967.552	0.01	8967.519	0.05	8967.491	0.07
0	1	3	12520.12	12520.153	-0.03	12520.089	0.03	12520.068	0.06
0	2	0	3139.05	3138.999	0.05	3139.038	0.01	3139.031	0.02
0	2	1	6844.60	6844.580	0.02	6844.566	0.03	6844.539	0.06
0	2	2	10483.22	10483.264	-0.04	10483.202	0.02	10483.212	0.01
0	3	0	4648.48	4648.435	0.04	4648.469	0.01	4648.452	0.03
0	3	1	8341.11	8341.109	0.00	8341.086	0.02	8341.114	-0.01
0	3	2	11963.54	11963.580	-0.04	11963.507	0.03	11963.615	-0.08
0	4	0	6110.42	6110.408	0.02	6110.433	-0.01	6110.410	0.01
0	4	1	9795.33	9795.354	-0.02	9795.324	0.01	9795.329	0.00
1	0	0	3649.69	3649.688	0.00	3649.649	0.04	3649.667	0.02
1	0	1	7228.88	7228.934	-0.05	7228.883	0.00	7228.888	0.00
1	0	2	10839.96	10839.986	-0.03	10839.942	0.01	-	-
1	0	3	14276.34	14276.389	-0.05	14276.318	0.02	14276.229	0.11
1	1	0	5221.24	5221.233	0.01	5221.227	0.02	5221.298	-0.05
1	1	1	8779.72	8779.747	-0.03	8779.707	0.01	8779.722	0.00
1	1	2	12372.71	12372.723	-0.02	12372.679	0.03	-	-
1	2	0	6755.51	6755.528	-0.02	6755.483	0.03	6755.501	0.01
1	2	1	10295.63	10295.673	-0.04	10295.616	0.02	10295.524	0.11
1	3	0	8249.04	8249.063	-0.03	8249.023	0.01	8249.073	-0.04
1	3	1	11774.71	11774.742	-0.03	11774.701	0.01	11774.670	0.04
2	0	0	7185.88	7185.894	-0.02	7185.879	0.00	7185.880	0.00
2	0	1	10585.29	10585.357	-0.07	10585.292	-0.01	10585.300	-0.01
2	0	2	14187.98	14188.069	-0.09	14187.985	0.00	-	-
2	1	0	8739.53	8739.530	0.00	8739.520	0.01	8739.589	-0.06
2	1	1	12116.80	12116.851	-0.05	12116.778	0.02	12116.833	-0.04
2	2	0	10256.58	10256.604	-0.02	10256.569	0.02	10256.537	0.05
2	2	1	13612.71	13612.745	-0.04	13612.688	0.02	13612.468	0.24
2	3	0	11734.53	11734.543	-0.02	11734.517	0.01	11734.625	-0.10
3	0	0	10573.92	10573.955	-0.04	10573.927	-0.01	10573.898	0.02
3	0	1	13795.40	13795.455	-0.06	13795.410	-0.01	13795.280	0.12
3	1	0	12106.98	12107.025	-0.05	12106.974	0.00	12107.006	-0.03
3	2	1	16775.38	16775.396	-0.01	16775.385	0.00	16774.779	0.60
4	0	1	16854.99	16855.126	-0.14	16855.099	-0.11	16854.534	0.46

state, J , in the calculation was taken as $J = 50$ and the limiting energy as $30\,000\,\text{cm}^{-1}$. Analysis using the H_2^{16}O partition function (Vidler & Tennyson 2000) performed in BT2 suggests that these parameters are sufficient to cover all transitions longwards of $0.5\,\mu\text{m}$ for temperatures up to 3000 K.

Wavefunctions were obtained by solving the nuclear Schrödinger equation using two-step procedure of calculation of rovibrational energies (Tennyson & Sutcliffe 1986). The calculations benefitted from recent algorithmic improvements (Tennyson & Yurchenko 2016), in particular in the method used to construct the final Hamiltonian matrices for $J > 0$ due to Azzam et al. (2016). Transition intensities were computed for $\Delta J = 0$ and 1 for all four symmetries and every $J \leq 50$. The matrix elements of the DMS were calculated using the program DIPOLE of the suite DVR3D and the actual spectrum for both isotopologues was generated with the program Spectra. About 500 million transitions were calculated for each isotopologue.

Figure 1 shows the distribution of the H_2^{18}O lines in HotWat78.

Using our calculations we provide the values of partition function for both isotopologues for wide range of temperatures, which are presented in the Table 5 as well as in the supplementary data on a grid of 1 K. We use the HITRAN convention (Fischer et al. 2003) and include the nuclear statistical weights g_{ns} in to the partition function explicitly (Tennyson et al. 2016). The nuclear statistical weights for H_2^{18}O are the same as for the main isotopologue, 1 and 3 for the para- and ortho-states, respectively. In case of H_2^{17}O , g_{ns} are 6 (para) and 18 (ortho). For calculation of partition functions for H_2^{18}O and H_2^{17}O we used all available energy levels with applying the cut-off at $30000\,\text{cm}^{-1}$.

Table 3. Standard deviation in cm^{-1} with which our pseudo-experimental energy levels the of $H_2^{17}\text{O}$ and $H_2^{18}\text{O}$ predicted the observed ones compiled by Tennyson et al. (2010) as a function of rotational state, J , N is number of levels used for calculation of the standard deviation.

J	N	$H_2^{17}\text{O}$	N	$H_2^{18}\text{O}$
0	27	0.0058	39	0.0092
1	93	0.0056	124	0.0093
2	161	0.0071	212	0.0109
3	199	0.0074	254	0.0090
4	236	0.0118	316	0.0147
5	232	0.0103	335	0.0141
6	263	0.0100	401	0.0116
7	222	0.0138	385	0.0140
8	182	0.0146	381	0.0130
9	138	0.0123	335	0.0174
10	116	0.0130	288	0.0176
11	72	0.0080	232	0.0168
12	47	0.0111	188	0.0201
13	26	0.0083	135	0.0179
14	9	0.0096	106	0.0198
15	3	0.0150	73	0.0176
16	1	0.0066	46	0.0184
17	1	0.0015	19	0.0156
18			11	0.0187

Table 4. Prediction of experimental energy levels of $H_2^{18}\text{O}$. Experimental (obs) data is taken from Makarov et al. (2015).

J	Observed	Calculated	Obs.-Calc.
0	27476.33	27476.24	0.09
1	27497.03	27496.92	0.11
1	27510.64	27510.31	0.33
1	27517.09	27517.44	-0.35
2	27537.12	27536.96	0.16
2	27546.82	27546.45	0.37
1	27509.55	27509.19	0.36
2	27545.66	27545.28	0.38

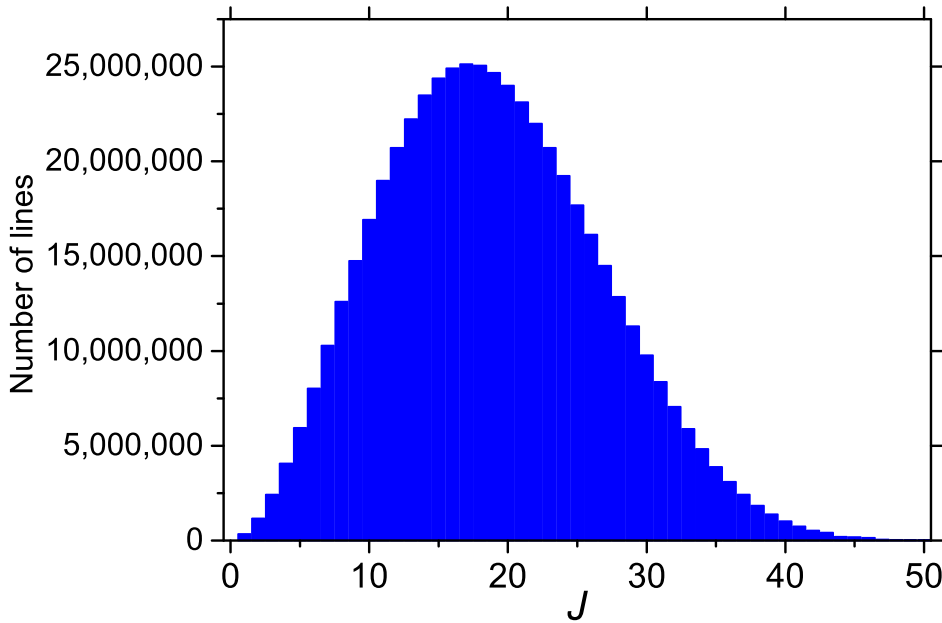


Figure 1. The distribution of the $H_2^{18}\text{O}$ transitions per J in the line HotWat78 list.

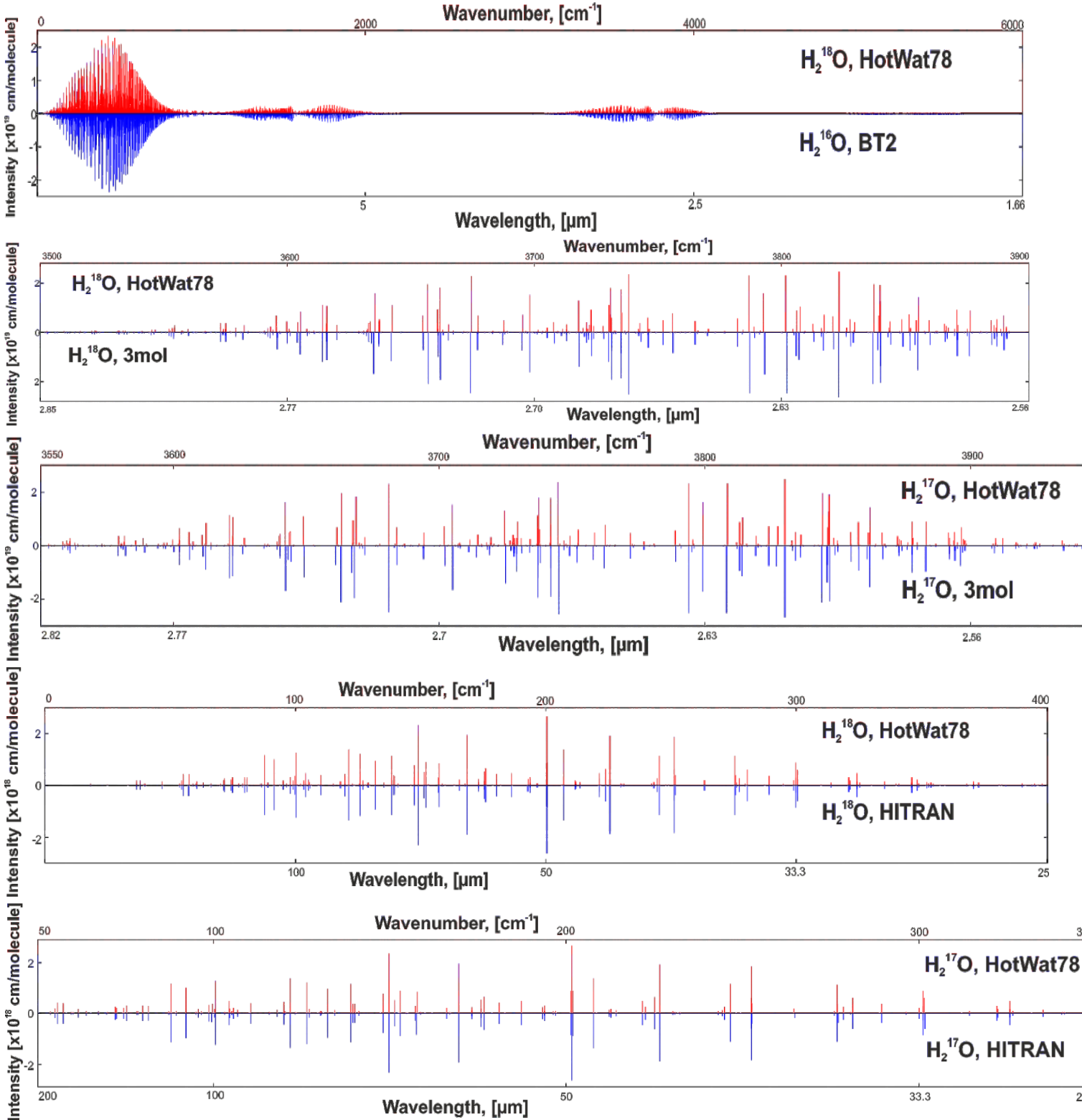


Figure 2. Comparison between BT2 and HotWat78 for H_2^{18}O at the temperature $T=2000$ K, and comparison of HotWat78 with 3mol (Shirin et al. 2008) and HITRAN at $T=296$ K for H_2^{18}O and H_2^{17}O respectively.

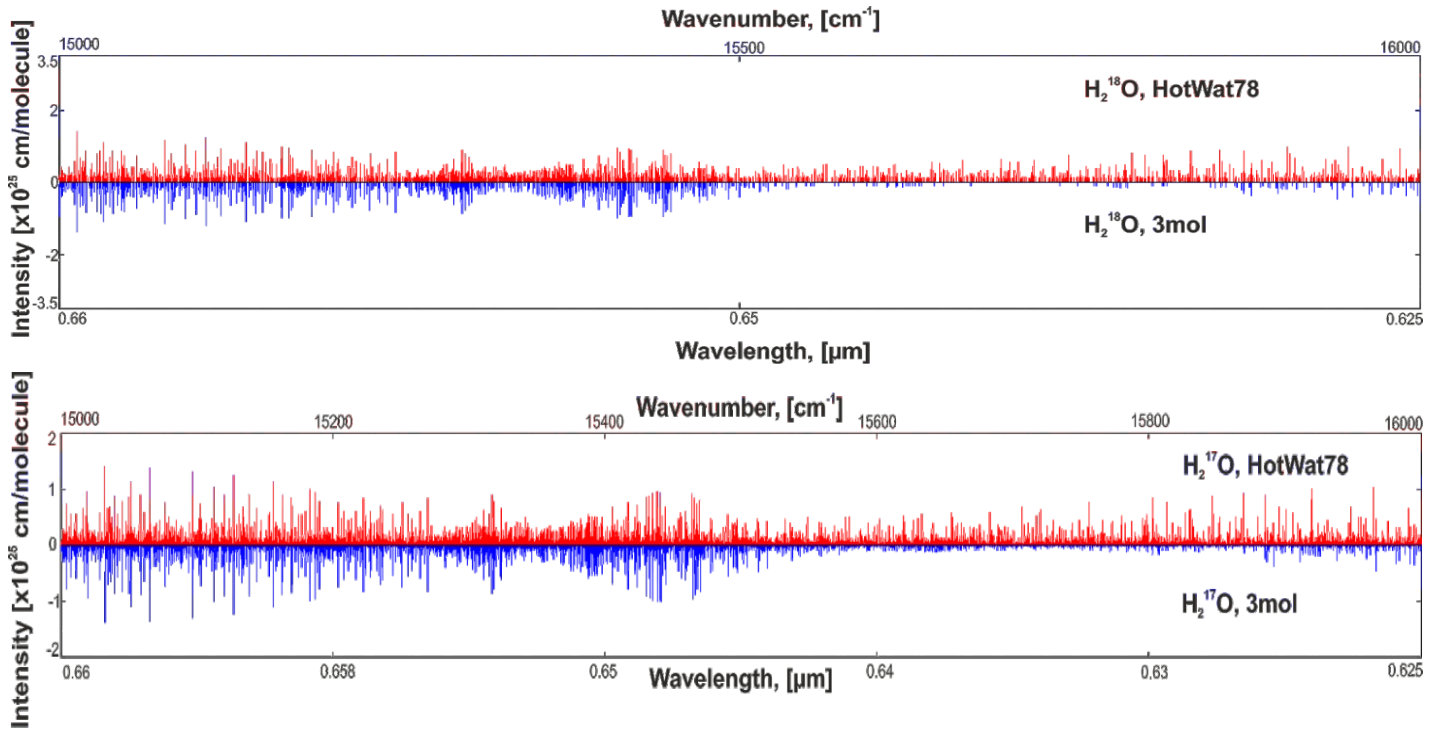


Figure 3. Comparison of $H_2^{18}O$ and $H_2^{17}O$ between 3mol (Shirin et al. 2008) and HotWat78 at the temperature $T=3000$ K.

4 IMPROVED PSEUDO-EXPERIMENTAL ENERGY LEVELS

The series of IUPAC papers on the various isotopologues of water (Tennyson et al. 2009, 2010, 2013, 2014) used measured transition frequencies to derive ro-vibrational energy levels using the so-called MARVEL (measured active rotation-vibration energy levels) procedure (Furtenbacher et al. 2007; Furtenbacher & Császár 2012). These energy levels can be used to generate pseudo-experimental values of the line frequencies in our line lists when the calculated energy level is substituted by the corresponding (pseudo-)experimental one. The comparison of these generated line frequencies with actual experimental ones demonstrate near-perfect coincidence. The number of generated pseudo-experimental lines is significantly higher than the number of the directly observed lines because line frequencies between pseudo-experimental levels can be predicted to high accuracy even when the lines have not been measured, as demonstrated by Tennyson et al. (2013). Less than 200 000 experimentally observed $H_2^{16}O$ lines give rise to about 5 000 000 lines with pseudo-experimental frequencies generated in this way. Use of such a procedure provides significantly more accurate line lists than just the calculated ones. We therefore substituted our computed energy with those of Tennyson et al. (2009) where possible.

However as described in section 2, the procedure for fitting PES using $H_2^{16}O$ data opens the way for us to further improve the accuracy of the calculated line lists. Looking at Table 6, we can see that the obs–calc residuals for a particular $H_2^{16}O$ vibrational state are very similar to the residuals for the same states of $H_2^{17}O$ and $H_2^{18}O$. The following procedure can be used to exploit this. First let us consider the idealised situation when all the residuals for energy levels of $H_2^{16}O$, $R_{v,J}(16)$, are exactly equal to those of $H_2^{18}O$, $R_{v,J}(18)$, where (v, J) represent the vibrational and rotational quantum numbers. In this case we can predict the precise “estimated” value of an $H_2^{18}O$ level, $E_{v,J}^{\text{est}}(18)$, from the empirically-determined levels of $H_2^{16}O$, $E_{v,J}^{\text{obs}}(18)$

$$E_{v,J}^{\text{est}}(18) = E_{v,J}^{\text{calc}}(18) + R_{v,J}(18) = E_{v,J}^{\text{calc}}(18) + R_{v,J}(16) \quad (1)$$

where $E_{v,J}^{\text{calc}}(18)$ is the corresponding calculated $H_2^{18}O$ energy level. So even if the level of the $H_2^{18}O$ isotopologue has yet to be observed, its pseudo-experimental value can be retrieved from the calculated level of $H_2^{18}O$ using our calculations plus the residual for $H_2^{16}O$ provided the experimental level of $H_2^{16}O$ is known.

Table 6 shows that residuals for $H_2^{16}O$ and $H_2^{18}O$ are slightly different, we can therefore improve this procedure. We notice from the Table 6, that the $H_2^{16}O$ and $H_2^{18}O$ residuals differ by similar amounts. If we average this value:

$$\Delta R(18) = \frac{1}{N} \sum_{v=1}^N R_{v,0}(18) - R_{v,0}(16). \quad (2)$$

Table 5. Partition Function of H₂¹⁷O and H₂¹⁸O.

T(K)	H ₂ ¹⁷ O	H ₂ ¹⁸ O
10	7.97970859	1.33135007
20	20.1629004	3.37074465
40	56.7292812	9.48860674
60	101.331587	16.9509639
80	153.237432	25.6357152
100	211.822453	35.4382143
200	587.053283	98.2237727
296	1052.12202	176.043783
300	1073.45356	179.613285
400	1654.78625	276.895547
500	2328.51505	389.655412
600	3099.26294	518.674912
800	4966.65892	831.352302
1000	7346.85187	1230.02825
1200	10357.5304	1734.46724
1400	14140.2160	2368.43292
1500	16371.1820	2742.40404
1600	18857.9004	3159.29345
1800	24694.5428	4137.93895
2000	31855.8230	5338.90908
2200	40570.4778	6800.61746
2400	51091.7815	8565.59949
2500	57116.1119	9576.29200
2600	63698.8388	10680.7274
2800	78697.3411	13197.3344
3000	96419.4218	16171.1873
3200	117222.299	19662.2543
3400	141485.523	23734.2409
3500	155038.487	26008.8411
3600	169606.832	28453.8904
3800	201996.792	33890.0829
4000	239072.534	40112.7834
4200	281250.969	47191.9028
4400	328941.890	55196.1417
4500	354979.000	59566.0429
4600	382541.321	64191.8753
4800	442425.403	74242.1299
5000	508945.054	85405.6885
5200	582421.516	97736.3470
5400	663142.877	111282.333
5500	706300.716	118524.515
5600	751361.549	126085.883
5800	847292.676	148990.861
6000	951113.377	159603.233

where N runs over the number of vibrational states for which $J = 0$ levels are known, which corresponds to 40 for H₂¹⁷O and 24 for H₂¹⁸O. Then we can use this average difference to further correct our estimated H₂¹⁸O energy levels using the revised formula:

$$E_{v,j}^{\text{est}}(18) = E_{v,J}^{\text{calc}}(18) + R_{v,J}(16) + \Delta R(18). \quad (3)$$

Calculating the observed values of energies of H₂¹⁸O using Eq. (1) gives a standard deviation for $E_{v,j}^{\text{est}}(18)$ levels from the known experimental values, $E_{v,j}^{\text{obs}}(18)$, of 0.009 cm⁻¹. However, $\Delta R(18)$ is 0.006 cm⁻¹. If instead we use Eq. (3), then the standard deviation reduces to 0.003 cm⁻¹. Although $\Delta R(18)$ is evaluated for $J = 0$ only, this procedure still works for higher J values. For example it also results in a standard deviation of 0.003 cm⁻¹ when applied to the $J = 10$ levels of the (010) state.

This procedure, which can clearly also be applied to H₂¹⁷O, leads to the generation of about 5 million transitions which involve the pseudo-experimental levels of H₂¹⁷O and H₂¹⁸O. It therefore provides a line list with much more accurate values of the frequencies of these transitions: in general better by about 0.005 cm⁻¹ for H₂¹⁷O and somewhat worse for H₂¹⁸O, but still much more accurate than possible with variational calculations.

The reason this procedure can be applied to the construction of the pseudo-experimental values of the energy levels of minor isotopologues is that for the major water isotopologue H₂¹⁶O the number of energy levels known experimentally is

Table 6. Vibrational band origins, in cm^{-1} , for $H_2^{16}\text{O}$, $H_2^{17}\text{O}$ and $H_2^{18}\text{O}$. Observed (obs) data is taken from Tennyson et al. (2013) and Tennyson et al. (2009); calculated results are given as observed minus calculated (o–c).

$(v_1 v_2 v_3)$	$H_2^{16}\text{O}$		$H_2^{17}\text{O}$		$H_2^{18}\text{O}$	
	obs	o–c	obs	o–c	obs	o–c
(010)	1594.75	0.019	1591.33	0.028	1588.28	0.036
(020)	3151.63	0.040	3144.98	0.046	3139.05	0.051
(100)	3657.05	-0.007	3653.14	-0.005	3649.69	-0.002
(110)	5234.97	0.005	5227.71	0.014	5221.24	0.010
(120)	6775.09	-0.028	6764.73	-0.022	6755.51	-0.018
(200)	7201.54	-0.024	7193.25	-0.019	7185.88	-0.016
(012)	9000.14	-0.009	8982.87	0.001	8967.57	0.013
(102)	10868.88	-0.049	10853.51	-0.040	10839.96	-0.030
(001)	3755.93	-0.017	3748.32	-0.015	3741.57	-0.014
(011)	5331.27	-0.002	5320.25	0.010	5310.46	0.019
(021)	6871.52	0.004	6857.27	0.012	6844.60	0.019
(101)	7249.82	-0.063	7238.71	-0.059	7228.88	-0.051
(111)	8807.00	-0.044	8792.54	-0.034	8779.72	-0.027
(121)	10328.73	-0.055	10311.20	-0.045	10295.63	-0.039
(201)	10613.36	-0.074	10598.48	-0.075	10585.29	-0.072
(003)	11032.40	-0.061	11011.88	-0.053	10993.68	-0.053
(131)	11813.20	-0.041	11792.82	-0.039	11774.71	-0.034
(211)	12151.25	-0.072	12132.99	-0.064	12116.80	-0.054
(113)	12565.01	-0.050	12541.23	-0.041	12520.12	-0.030
(221)	13652.66	-0.045	13631.50	-0.042	13612.71	-0.035
(301)	13830.94	-0.062	13812.16	-0.057	13795.40	-0.057
(103)	14318.81	-0.069	14296.28	-0.061	14276.34	-0.053

significantly higher, than that for $H_2^{17}\text{O}$ and $H_2^{18}\text{O}$. For example the assignment of weak $H_2^{16}\text{O}$ lines in various regions is available (Tolchenov et al. 2005; Polyansky et al. 1998; Schermaul et al. 2002), where isotopologues data are not known. As a result very highly-excited bending (Polyansky et al. 1997; Zobov et al. 2005) and stretching energy levels (Maksyutenko et al. 2007; Grechko et al. 2009; Császár et al. 2010) are known, which form the basis upon which our pseudo-experimental energy levels are constructed.

5 RESULTS

The newly constructed $H_2^{17}\text{O}$ and $H_2^{18}\text{O}$ line lists are named HotWat78. The new HotWat78 line lists are calculated for $J \leq 50$ and for the spectral range $0\text{--}30000 \text{ cm}^{-1}$. HotWat78 contains 519 461 789 lines for $H_2^{18}\text{O}$ is 519 461 789 and 513 112 779 lines for $H_2^{17}\text{O}$. The new linelist is both the most complete and the most accurate one, see Tables 1 and 2. They are stored in the ExoMol format (Tennyson et al. 2013) which uses the compact storage of results originally developed for BT2. This involves using a states file (`.states`), see Table 7, and a transitions file (`.trans`), see Table 8. The energy levels in the states files are marked as ‘observed’ if the results are taken from the IUPAC compilation, ‘estimated’ if they are generated using Eq. (3) or as ‘calculated’, for which the results of the PES2 calculation are used.

The states file lists all the ro-vibrational levels for each J and for four C_{2v} symmetries. It is common to further label the every level with (approximate) vibrational quantum numbers (v_1, v_2, v_3) which correspond to the symmetric stretch, bending and asymmetric stretch modes, respectively and the Rotational levels within each vibrational state by J, K_a, K_c , where again the projection quantum numbers K_a and K_c are approximate. DVR3D does not provide these approximate labels but there are several methods available for labeling water energy levels (Partridge & Schwenke 1997; Szidarovszky et al. 2012; Shirin et al. 2008). Here we label levels with $J \leq 20$ and energies below $20\,000 \text{ cm}^{-1}$. As our energy levels differ by less than 1 cm^{-1} from those of Shirin et al. (2008), transferring the labels from this previous study proved to be straightforward. We note that the labels we use are based on the normal modes from a harmonic oscillator model. It is well known that the higher stretching states of water are better represented with a local-mode model (Child & Halonen 1984). However, there is a one-to-one correspondance between the two labelling schemes (Carleer et al. 1999); the use of normal mode labels are used for simplicity.

The accuracy of the present line lists can be established by the comparison with the previous line lists calculations. Two types of comparison could be made. The overall picture for the high temperature is that the coverage the HotWat78 $H_2^{17}\text{O}$ and $H_2^{18}\text{O}$ line lists should be very similar to BT2, but that both the predicted intensives and the line positions should be significantly better. Furthermore lines may shift by between a few cm^{-1} to a few tens of cm^{-1} between isotopologues. Figure 1 demonstrate that, as expected, the overall picture is very similar for BT2 ($H_2^{16}\text{O}$) and HotWat78 ($H_2^{17}\text{O}$ and $H_2^{18}\text{O}$). Here we provide the comparison only for $H_2^{18}\text{O}$ but for the $H_2^{17}\text{O}$ it looks the same.

Table 7. Extract from the final states file for H_2^{17}O .

<i>i</i>	\tilde{E}	g_{tot}	<i>J</i>	K_a	K_c	v1	v2	v3	<i>S</i>
1	0.000000	6	0	0	0	0	0	0	A1
2	1591.322876	6	0	0	0	0	1	0	A1
3	3144.980225	6	0	0	0	0	2	0	A1
4	3653.145752	6	0	0	0	1	0	0	A1
5	4657.115211	6	0	0	0	0	3	0	A1
6	5227.703125	6	0	0	0	1	1	0	A1
7	6121.557129	6	0	0	0	0	4	0	A1
8	6764.726562	6	0	0	0	1	2	0	A1
9	7193.246582	6	0	0	0	2	0	0	A1
10	7431.093262	6	0	0	0	0	0	2	A1
11	7527.489258	6	0	0	0	0	5	0	A1
12	8260.781250	6	0	0	0	1	3	0	A1
13	8749.905273	6	0	0	0	2	1	0	A1
14	8853.288086	6	0	0	0	0	6	0	A1
15	8982.860352	6	0	0	0	0	1	2	A1
16	9708.538086	6	0	0	0	1	4	0	A1
17	10068.091797	6	0	0	0	0	7	0	A1
18	10269.661133	6	0	0	0	2	2	0	A1
19	10501.353516	6	0	0	0	0	2	2	A1
20	10586.049805	6	0	0	0	3	0	0	A1

i: State counting number.

\tilde{E} : State energy in cm^{-1} .

g: Total state degeneracy.

J: Total angular momentum

K_a : Asymmetric top quantum number.

K_c : Asymmetric top quantum number.

ν_1 : Symmetric stretch quantum number.

ν_2 : Bending quantum number.

ν_3 : Asymmetric stretch quantum number.

S: State symmetry in C_{2v} .

Figures 2 and 3 illustrate the similarity of the HotWat78 line lists with the previous high accuracy H_2^{17}O and H_2^{18}O line lists (called 3mol) of Shirin et al. (2008) for these molecules at the room temperature. Figures 4 and 5 also provide a comparison with the HITRAN data for the room temperature for H_2^{17}O and H_2^{18}O . These figures only provide an overview, but a detailed line by line comparison confirms that all the calculations we present here are done correctly.

The present line lists are significantly more complete, but this is only apparent at higher temperatures, see Fig. 3. For the room temperature the previous line lists should look similar, as they indeed do, see Figures 2.

6 CONCLUSIONS

This paper reports hot line lists for H_2^{17}O and H_2^{18}O . These line lists represent significant improvement on both coverage and accuracy of the previous H_2^{17}O and H_2^{18}O line lists (Mikhailenko et al. 2005; Shirin et al. 2008). The predicted frequencies in these line lists have been significantly improved using information obtained from the corresponding H_2^{16}O empirical energy levels. This procedure can be adapted to give improved predictions of energy levels and transition frequencies for isotopologues of molecules for whom the empirical energy levels of the parent molecule are well-known.

The complete HotWat78 line lists for H_2^{17}O and H_2^{18}O can be downloaded from the CDS, via <ftp://cdsarc.u-strasbg.fr/pub/cats/J/MNRAS/>, or via <http://cdsarc.u-strasbg.fr/viz-bin/qcat?J/MNRAS/>. The line lists together with auxiliary data including the potential parameters, dipole moment functions, and theoretical energy levels can be also obtained at www.exomol.com, where they form part of the enhanced Exomol database (Tennyson et al. 2016). The BT2 H_2^{16}O line list (Barber et al. 2006) is already available from these sources.

Finally we note that pressure-broadening has been shown to have a significant effect on water spectra in exoplanets (Tinetti et al. 2012). ExoMol, in common with other databases, assumes that pressure-broadening parameters for H_2^{17}O and H_2^{18}O are the same as those for H_2^{16}O . This assumption is built into the recently updated structure of the ExoMol database (Tennyson et al. 2016). Barton et al. (2016) have recently presented a comprehensive set of pressure-broadening parameters for H_2^{16}O lines which form the basis for the ExoMol pressure-broadening diet for water (Barton et al. 2016). These parameters, which are available on the ExoMol website, are also suitable for use with the HotWat78 line lists.

Table 8. Extract from the transitions file for $H_2^{17}O$

f	i	A_{fi}
142344	150189	5.6651e-05
2235	2362	1.7434e-03
34497	35342	5.7700e-09
125681	114596	5.5394e-10
135143	128340	6.3329e-08
24055	16736	1.5208e-03
147918	137719	1.3405e-04
45027	45537	8.0306e-07
37457	31884	9.0168e-08
39192	43632	7.3676e-07
25153	26085	4.3393e-05
131146	124272	8.5679e-04
134840	128287	8.5680e-04
88744	94220	1.2221e-03
102017	106580	2.4131e-04
193489	187074	2.7697e-06
202910	204558	7.0571e-03
53725	50906	1.8345e-06
142862	135857	2.5908e-05

f : Upper state counting number.

i : Lower state counting number.

A_{fi} : Einstein-A coefficient in s^{-1} .

ACKNOWLEDGEMENTS

This work is supported by ERC Advanced Investigator Project 267219 and by the Russian Fund for Fundamental Studies.

REFERENCES

- Abia C., Palmerini S., Busso M., Cristallo S., 2012, A&A, 548, A55
 Allard F., 2014, in Booth M., Matthews B. C., Graham J. R., eds, IAU Symposium Vol. 299 of IAU Symposium, The BT-Settl Model Atmospheres for Stars, Brown Dwarfs and Planets. pp 271–272
 Azzam A. A. A., Yurchenko S. N., Tennyson J., Naumenko O. V., 2016, MNRAS, 460, 4063
 Bailey J., 2009, Icarus, 201, 444
 Banerjee D. P. K., Barber R. J., Ashok N. K., Tennyson J., 2005, ApJ, 627, L141
 Barber R. J., Miller S., Dello Russo N., Mumma M. J., Tennyson J., Guio P., 2009, MNRAS, 398, 1593
 Barber R. J., Tennyson J., Harris G. J., Tolchenov R. N., 2006, MNRAS, 368, 1087
 Barton E. J., Hill C., Czurylo M., Li H.-Y., Hyslop A., Yurchenko S. N., Tennyson J., 2016, J. Quant. Spectrosc. Radiat. Transf.
 Barton E. J., Hill C., Yurchenko S. N., Tennyson J., Dudaryonok A., Lavrentieva N. N., 2016, J. Quant. Spectrosc. Radiat. Transf., p. (in press)
 Birkby J. L., de Kok R. J., Brogi M., de Mooij E. J. W., Schwarz H., Albrecht S., Snellen I. A. G., 2013, MNRAS, 436, L35
 Bubukina I. I., Polyansky O. L., Zobov N. F., Yurchenko S. N., 2011, Optics and spectroscopy, 110, 160
 Bykov A. D., Lavrentieva N. N., Mishina T. P., Sinitsa L. N., Barber R. J., Tolchenov R. N., Tennyson J., 2008, J. Quant. Spectrosc. Radiat. Transf., 109, 1834
 Carleer M., Jenouvrier A., Vandaele A.-C., Bernath P. F., Mérienne M. F., Colin R., Zobov N. F., Polyansky O. L., Tennyson J., Savin V. A., 1999, J. Chem. Phys., 111, 2444
 Chesnokova T. Y., Voronin B. A., Bykov A. D., Zhuravleva T. B., Kozodoev A. V., Lugovskoy A. A., Tennyson J., 2009, J. Mol. Spectrosc., 256, 41
 Child M. S., Halonen L., 1984, Adv. Chem. Phys., 57, 1
 Clayton R. N., Mayeda T. K., 1984, Earth Planet. Sci. Lett., 67, 151
 Császár A. G., Mátyus E., Lodi L., Zobov N. F., Shirin S. V., Polyansky O. L., Tennyson J., 2010, J. Quant. Spectrosc. Radiat. Transf., 111, 1043
 Dello Russo N., Bonev B. P., DiSanti M. A., Gibb E. L., Mumma M. J., Magee-Sauer K., Barber R. J., Tennyson J., 2005, ApJ, 621, 537
 Dello Russo N., DiSanti M. A., Magee-Sauer K., Gibb E. L., Mumma M. J., Barber R. J., Tennyson J., 2004, Icarus, 168, 186

- Fischer J., Gamache R. R., Goldman A., Rothman L. S., Perrin A., 2003, *J. Quant. Spectrosc. Radiat. Transf.*, 82, 401
- Floss C., Stadermann F. J., Mertz A. F., Bernatowicz T. J., 2010, *Meteoritics Planet. Sci.*, 45, 1889
- Furtenbacher T., Császár A. G., 2012, *J. Quant. Spectrosc. Radiat. Transf.*, 113, 929
- Furtenbacher T., Császár A. G., Tennyson J., 2007, *J. Mol. Spectrosc.*, 245, 115
- Grechko M., Boyarkin O. V., Rizzo T. R., Maksyutenko P., Zobov N. F., Shirin S., Lodi L., Tennyson J., Császár A. G., Polyansky O. L., 2009, *J. Chem. Phys.*, 131, 221105
- Kranendonk L. A., An X., Caswell A. W., Herold R. E., Sanders S. T., Huber R., Fujimoto J. G., Okura Y., Urata Y., 2007, *Optics Express*, 15, 15115
- Lampel J., Pöhler D., Polyansky O. L., Kyuberis A. A., Zobov N. F., Tennyson J., Lodi L., Frieß U., Wang Y., Beirle S., Platt U., Wagner T., 2016, *Atmos. Chem. Phys.*
- Lodi L., Tennyson J., 2012, *J. Quant. Spectrosc. Radiat. Transf.*, 113, 850
- Lodi L., Tennyson J., Polyansky O. L., 2011, *J. Chem. Phys.*, 135, 034113
- Lodi L., Tolchenov R. N., Tennyson J., Lynas-Gray A. E., Shirin S. V., Zobov N. F., Polyansky O. L., Császár A. G., van Stralen J., Visscher L., 2008, *J. Chem. Phys.*, 128, 044304
- Makarov D. S., Koshelev M. A., Zobov N. F., Boyarkin O. V., 2015, *Chem. Phys. Lett.*, 627, 73
- Maksyutenko P., Muenter J. S., Zobov N. F., Shirin S. V., Polyansky O. L., Rizzo T. R., Boyarkin O. V., 2007, *J. Chem. Phys.*, 126, 241101
- Mathar R. J., 2007, *J. Optics A*, 9, 470
- Matsuura M., Yates J. A., Barlow M. J., Swinyard B. M., Royer P., Cernicharo J., Decin L., Wesson R., Polehampton E. T., Blommaert J. A. D. L., Groenewegen M. A. T., de Steene G. C. V., Van Hoof P. A. M., 2014, *MNRAS*, 437, 532
- Mikhailenko S. N., Babikov Y. L., F. G. V., 2005, *Atmospheric and Oceanic Optics*, 18, 685
- Neufeld D. A., Tolls V., Agundez M., Gonzalez-Alfonso E., Decin L., Daniel F., Cernicharo J., Melnick G. J., Schmidt M., Szczerba R., 2013, *ApJ*, 767, L3
- Nittler L. R., Gaidos E., 2012, *Meteoritics Planet. Sci.*, 47, 2031
- Partridge H., Schwenke D. W., 1997, *J. Chem. Phys.*, 106, 4618
- Polyansky O. L., Császár A. G., Shirin S. V., Zobov N. F., Barletta P., Tennyson J., Schwenke D. W., Knowles P. J., 2003, *Science*, 299, 539
- Polyansky O. L., Jensen P., Tennyson J., 1994, *J. Chem. Phys.*, 101, 7651
- Polyansky O. L., Zobov N. F., Tennyson J., Lotoski J. A., Bernath P. F., 1997, *J. Mol. Spectrosc.*, 184, 35
- Polyansky O. L., Zobov N. F., Viti S., Tennyson J., 1998, *J. Mol. Spectrosc.*, 189, 291
- Rajpurohit A. S., Reyle C., Allard F., Scholz R. D., Homeier D., Schultheis M., Bayo A., 2014, *A&A*, 564, A90
- Rein K. D., Sanders S. T., 2010, *Appl. Optics*, 49, 4728
- Rice E. L., Barman T., Mclean I. S., Prato L., Kirkpatrick J. D., 2010, *ApJS*, 186, 63
- Rothman L. S., Gordon I. E., Barber R. J., Dothe H., Gamache R. R., Goldman A., Perevalov V. I., Tashkun S. A., Tennyson J., 2010, *J. Quant. Spectrosc. Radiat. Transf.*, 111, 2139
- Rothman L. S. et al. 2013, *J. Quant. Spectrosc. Radiat. Transf.*, 130, 4
- Schermaul R., Learner R. C. M., Canas A. A. D., Brault J. W., Polyansky O. L., Belmiloud D., Zobov N. F., Tennyson J., 2002, *J. Mol. Spectrosc.*, 211, 169
- Shirin S. V., Polyansky O. L., Zobov N. F., Barletta P., Tennyson J., 2003, *J. Chem. Phys.*, 118, 2124
- Shirin S. V., Polyansky O. L., Zobov N. F., Ovsyannikov R. I., Császár A. G., Tennyson J., 2006, *J. Mol. Spectrosc.*, 236, 216
- Shirin S. V., Zobov N. F., Ovsyannikov R. I., Polyansky O. L., Tennyson J., 2008, *J. Chem. Phys.*, 128, 224306
- Szidarovszky T., Fabri C., Császár A. G., 2012, *J. Chem. Phys.*, 136, 174112
- Tennyson J., Bernath P. F., Brown L. R., Campargue A., Carleer M. R., Császár A. G., Daumont L., Gamache R. R., Hodges J. T., Naumenko O. V., Polyansky O. L., Rothman L. S., Vandaele A. C., Zobov N. F., Al Derzi A. R., Fábi C., Fazliev A. Z., Furtenbacher T., Gordon I. E., Lodi L., Mizus I. I., 2013, *J. Quant. Spectrosc. Radiat. Transf.*, 117, 29
- Tennyson J., Bernath P. F., Brown L. R., Campargue A., Carleer M. R., Császár A. G., Daumont L., Gamache R. R., Hodges J. T., Naumenko O. V., Polyansky O. L., Rothman L. S., Toth R. A., Vandaele A. C., Zobov N. F., Fazliev A. Z., Furtenbacher T., Gordon I. E., Mikhailenko S. N., Voronin B. A., 2010, *J. Quant. Spectrosc. Radiat. Transf.*, 111, 2160
- Tennyson J., Bernath P. F., Brown L. R., Campargue A., Carleer M. R., Császár A. G., Gamache R. R., Hodges J. T., Jenouvrier A., Naumenko O. V., Polyansky O. L., Rothman L. S., Toth R. A., Vandaele A. C., Zobov N. F., Daumont L., Fazliev A. Z., Furtenbacher T., Gordon I. E., Mikhailenko S. N., Shirin S. V., 2009, *J. Quant. Spectrosc. Radiat. Transf.*, 110, 573
- Tennyson J., Bernath P. F., Brown L. R., Campargue A., Császár A. G., Daumont L., Gamache R. R., Hodges J. T., Naumenko O. V., Polyansky O. L., Rothman L. S., Vandaele A. C., Zobov N. F., Dénes N., Fazliev A. Z., Furtenbacher T., Gordon I. E., Hu S.-M., Szidarovszky T., Vasilenko I. A., 2014, *J. Quant. Spectrosc. Radiat. Transf.*, 142, 93
- Tennyson J., Bernath P. F., Brown L. R., Campargue A., Császár A. G., Daumont L., Gamache R. R., Hodges J. T.,

- Naumenko O. V., Polyansky O. L., Rothman L. S., Vandaele A. C., Zobov N. F., 2014, Pure Appl. Chem., 86, 71
- Tennyson J., Hill C., Yurchenko S. N., 2013, in 6th international conference on atomic and molecular data and their applications ICAMDATA-2012 Vol. 1545 of AIP Conference Proceedings, Data structures for ExoMol: Molecular line lists for exoplanet and other atmospheres. AIP, New York, pp 186–195
- Tennyson J., Kostin M. A., Barletta P., Harris G. J., Polyansky O. L., Ramanlal J., Zobov N. F., 2004, Comput. Phys. Commun., 163, 85
- Tennyson J., Sutcliffe B. T., 1986, Mol. Phys., 58, 1067
- Tennyson J., Yurchenko S. N., 2012, MNRAS, 425, 21
- Tennyson J., Yurchenko S. N., 2016, Intern. J. Quantum Chem., p. (in press)
- Tennyson J., Yurchenko S. N., Al-Refaie A. F., Barton E. J., Chubb K. L., Coles P. A., Diamantopoulou S., Gorman M. N., Hill C., Lam A. Z., Lodi L., McKemmish L. K., Na Y., Owens A., Polyansky O. L., Rivlin T., Sousa-Silva C., Underwood D. S., Yachmenev A., Zak E., 2016, J. Mol. Spectrosc., 327, 73
- Tinetti G., Tennyson J., Griffiths C. A., Waldmann I., 2012, Phil. Trans. Royal Soc. London A, 370, 2749
- Tinetti G., Vidal-Madjar A., Liang M.-C., Beaulieu J.-P., Yung Y., Carey S., Barber R. J., Tennyson J., Ribas I., Allard N., Ballester G. E., Sing D. K., Selsis F., 2007, Nature, 448, 169
- Tolchenov R. N., Naumenko O., Zobov N. F., Shirin S. V., Polyansky O. L., Tennyson J., Carleer M., Coheur P.-F., Fally S., Jenouvrier A., Vandaele A. C., 2005, J. Mol. Spectrosc., 233, 68
- Vidler M., Tennyson J., 2000, J. Chem. Phys., 113, 9766
- Villanueva G. L., Mumma M. J., Novak R. E., Kaeufl H. U., Hartogh P., Encrenaz T., Tokunaga A., Khayat A., Smith M. D., 2015, Science, 348, 218
- Viti S., Tennyson J., Polyansky O. L., 1997, MNRAS, 287, 79
- Vollmer C., Hoppe P., Brenker F. E., 2008, ApJ, 684, 611
- Voronin B. A., Tennyson J., Tolchenov R. N., Lugovskoy A. A., Yurchenko S. N., 2010, MNRAS, 402, 492
- Zobov N. F., Polyansky O. L., Le Sueur C. R., Tennyson J., 1996, Chem. Phys. Lett., 260, 381
- Zobov N. F., Shirin S. V., Polyansky O. L., Tennyson J., Coheur P.-F., Bernath P. F., Carleer M., Colin R., 2005, Chem. Phys. Lett., 414, 193